

Supporting Information to: The Hydrogen Dependent CO₂ reductase: the first completely CO-tolerant FeFe-Hase

Pierre Ceccaldi Kai Schuchmann Volker Müller Sean J. Elliott

1 Methods

Experimental setup. Expression and purification of HDCR was achieved as described previously,¹ and the experimental setup for electrochemistry was also conducted as described previously.^{2,3} All experiments were carried out under strict anaerobic conditions ($O_2 < 1$ ppm). To form the enzyme films, we polished the pyrolytic graphite-edge electrode (surface ≈ 3 mm²) with an alumina slurry (Buehler, 1 μ m), then we applied 0.4-0.8 μ L of a solution of HDCR (8 μ M) to the surface. Electrochemical buffers contained 5 mM of each of MES, sodium acetate, HEPES, TAPS and CHES and 0.1 M NaCl, titrated to pH values as indicated.

Data analysis. Electrochemical data (voltammetry and amperometry) were analyzed using QSoas⁴ (the source code is available free of charge at QSoas.org). The kinetic schemes were written in simple text files readable by QSoas, as follows. In QSoas the expression:

```
Active <=> [kin*I] [kout] Inactive
```

was used to simulate the reversible binding of CO and O₂, where "k_{in}" is the bimolecular rate constant of the binding of the inhibitor "I", and k_{out} is the rate constant of its release. The equation used to fit the transients of CO inhibition can be found in the supplementary information of ref⁵ (see equation 3 therein).

The rate constant of CO release from the enzyme k_{out} and its departure from the electrochemical cell τ_{CO} are not independent parameters and need an external control to estimate τ_{CO} independently. This was done by measuring direct O₂ reduction on graphite at low potential under constant hydrogen flow, where the variation of current is described by the following: $[O_2]_t = [O_2]_0 \times e^{-t/\tau_{O_2}}$.

In the case of an unimolecular, irreversible transformation like the deactivation reaction of an O₂-bound state, we added the following line to the script:

```
Inactive -> [k3] Dead
```

where "k₃" is the rate constant of the irreversible reaction. This two-step mechanism has no analytical solution: because the reaction of O₂ with the enzyme is slow on the time-scale of τ_{O_2} , the equilibrium between "Active" and "Inactive" states is not reached and the current must be calculated by numerical integration.^{6,7}

At high potential, the enzyme undergoes two reversible unimolecular inactivations, which each can be written as:

Active $\rightarrow [k_{inact}] [k_{react}]$ Inactive-b

this expression thus appears as many times as anaerobic (in)activation count distinct phenomena. Note that distinct inactive species and rate constants must have distinct names.

Desorption of the enzyme must also be accounted for and can be described as a unimolecular, irreversible process, as described above. For fitting the data in figure 3, the equations of current $i(t)$ were simply multiplied by the following exponential decay: $e^{-k_{loss} \times t}$.

2 pH dependence of catalytic bias

We consider the catalytic bias (β) as the ratio of apparent maximum rates for H₂ production and oxidation under given conditions (pH and H₂ pressure). the pH dependence of β follows a power law that can be written as follows:

$$\beta = \beta_{lim} \times [H^+]^\alpha \quad (1)$$

where β_{lim} is the catalytic bias at pH 0 and α the slope of $\beta = f(pH)$ (see main text Figure 1, inset). We plotted three slopes, one with $\alpha=1$ (*i.e.* $\beta \propto [H^+]$, illustrating the case where proton reduction is limited by substrate availability), and two with $\alpha = 0.5$, describing the pH dependence of β in HDCR for the two values of [H₂] = 10 and 100 %. This means that β directly depends on $\sqrt{[H^+]}$ under all conditions. The reason why proton availability tunes HDCR Hase activity independently of H₂ concentration (at least on the pH and [H₂] range probed here) remains elusive at the moment. Literature lacks similar systematic studies of the catalytic bias as a function of substrates concentrations H⁺ and H₂. As a consequence, we can not assign with full certainty whether α is meaningful. Our opinion is that α might be considered as a "fingerprint" of the catalytic bias of HDCR, and its value must relate to the relative affinity of H₂ and H⁺ for the active site.

3 Measure of residual [H₂] related to the determination of H₂ affinity

During the experiment presented in Figure 3, traces of H₂ are remaining in the electrochemical cell upon switching off its flow. This residual H₂ results in a remaining oxidation current at the minimum of [H₂] (main text Figure 3 at $t \approx 1600$ s). Such a residual concentration needs to be taken into account during data analysis and introduces a bias in the determination of K_M and K_i .

In equations 1 and 2 of the main text, [H₂] can be written as follows:

$$([H_2]_0 - [H_2]_\infty) \times e^{\frac{t_0-t}{\tau}} + [H_2]_\infty \quad (2)$$

where [H₂]₀ is the initial H₂ concentration, [H₂]_∞ the final concentration and τ the time-constant at which H₂ flows into the cell or escapes into the gas phase.

The concentration of dissolved H₂ can be determined independently by running a chronopotentiometry exper-

iment. This consists in monitoring the open circuit potential (OCP), that is the potential of the electrode when current is null because reduction and oxidation reaction occur at the same rate, thus equilibrate each other. In the case of hydrogenases, the OCP reads the reduction potential of the H^+/H_2 redox couple. Upon turning off the H_2 flow, OCP changes accordingly to H_2 concentration in the cell. Figure S1 shows two subsequent experiments, the measurement of OCP following the measurement of H_2 oxidation activity upon flushing H_2 out of the cell (grey and black traces, respectively). These two signals can be further simulated with either the Nernst equation of the H^+/H_2 redox couple: $E = -\ln\frac{[H^+]^2}{[H_2](t)}$ or equation 1 from main text. Residual $[H_2]_\infty$ determined with the ‘‘OCP’’ experiment can then be used as a benchmark for the measurement of the apparent H_2 affinity parameters, K_M and K_i .

4 Supplementary figures

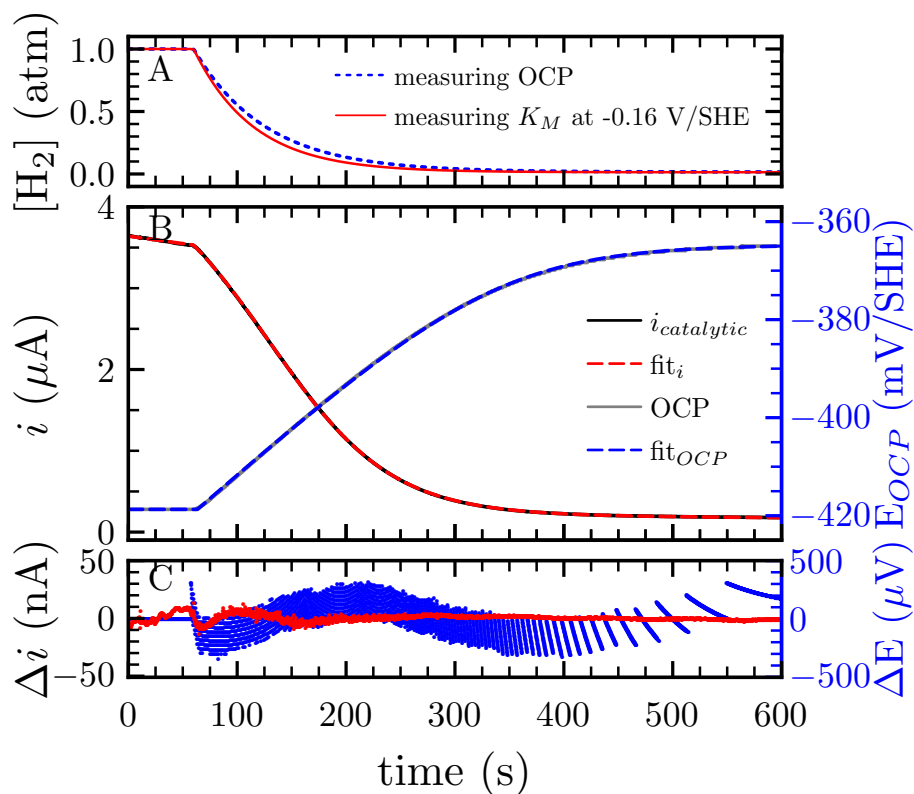


Figure S1: Measurement of K_M and residual H_2 at pH 7, 30°C. A. H_2 concentration against time, predicted from the fit of B. H_2 oxidation current at -160 mV/SHE (black) and Open Circuit Potential (grey) against time. Blue and red traces correspond to the best fit of parameters of equation 1 in main text, returning $K_M=0.23$ atm, time constant of H_2 escaping the cell is C. Fits residuals. $[H_2]_\infty = 13$ and $16 \mu\text{M}$, $\tau= 55$ and 66 s for the red and blue traces, respectively.

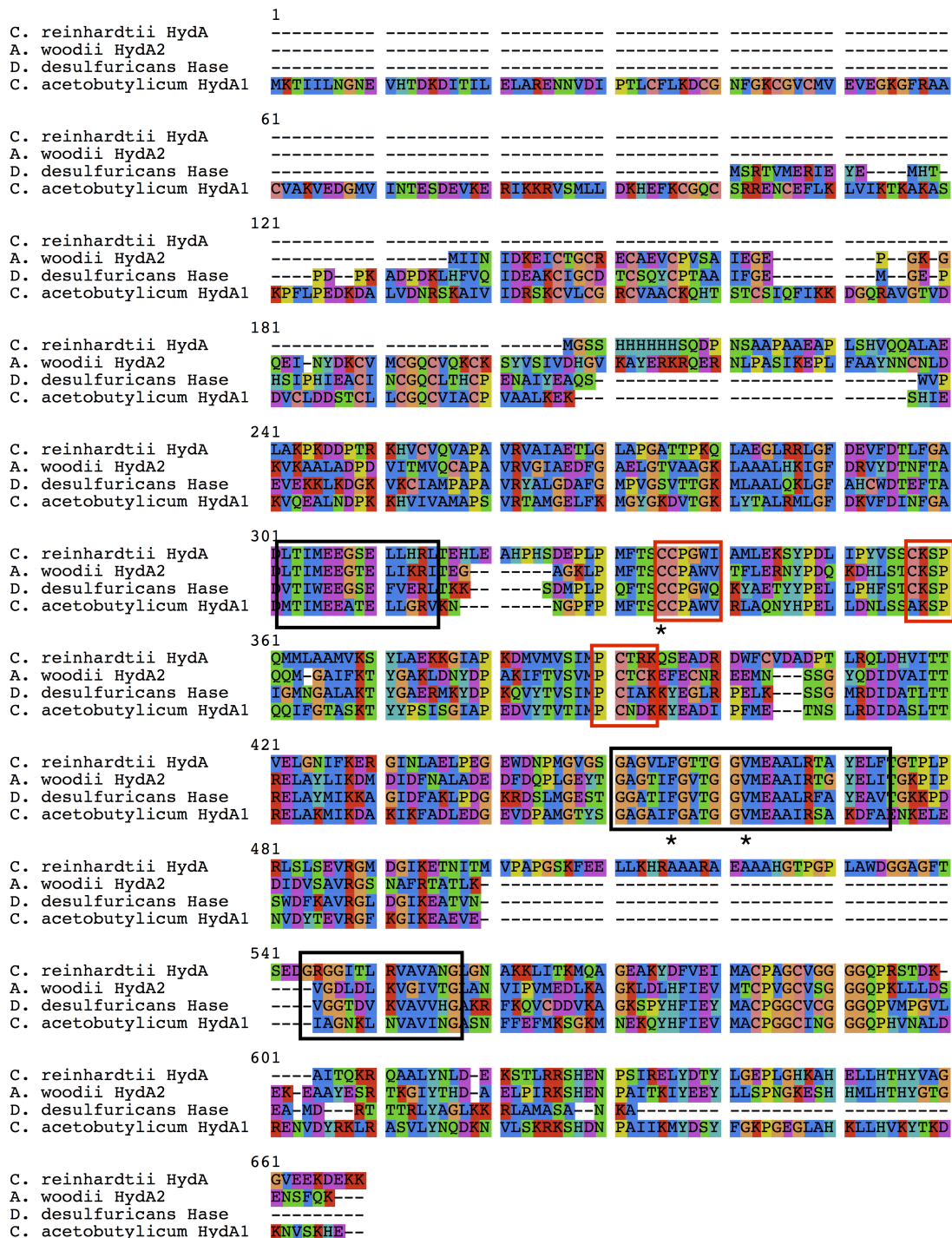


Figure S2: Multiple sequence alignment of archetypal FeFe-Hases with *A. woodii* HydA2. The squared regions correspond to the H-cluster cavity (red) and the substrate access tunnel (black). The starred positions correspond to the bottleneck of the gas tunnel shown in Figure S3. The sequences were aligned using the program *clustal*; the figure was produced with the software *Seaview*.

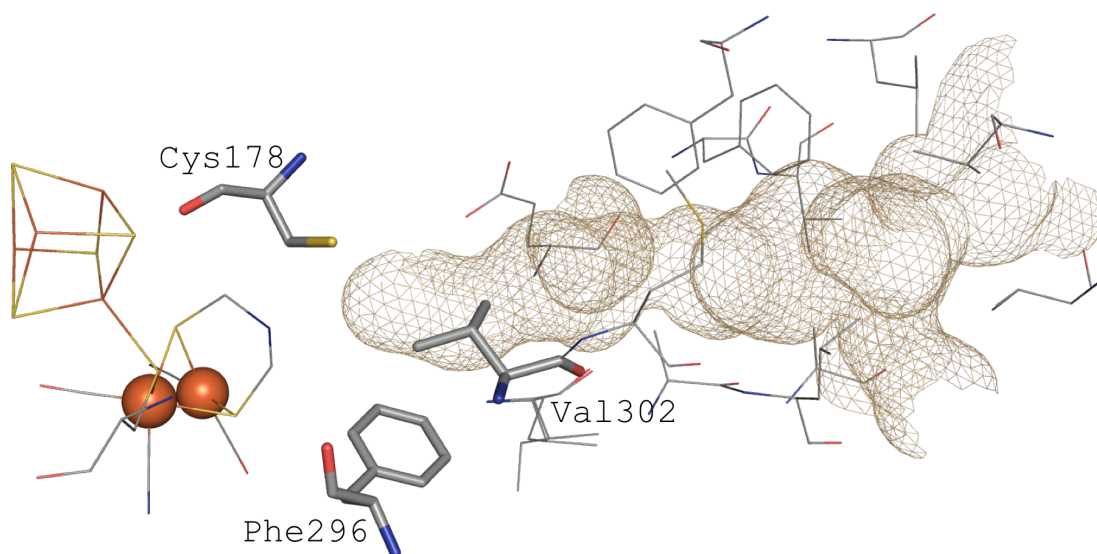


Figure S3: Residues shaping the substrate access tunnel in Dd-Hase, all of which are conserved in FeFe-Hases depicted in Figure S2. The residues shown in sticks (aa numbering from *Dd*-Hase⁸) form the gate to the active site, and have been targeted by mutagenesis studies in *Cr* or *Ca*-Hases.⁹⁻¹¹ The conserved residues (lines) shape the tunnel, shown in beige chicken-wire. The figure was produced using the software PyMOL.

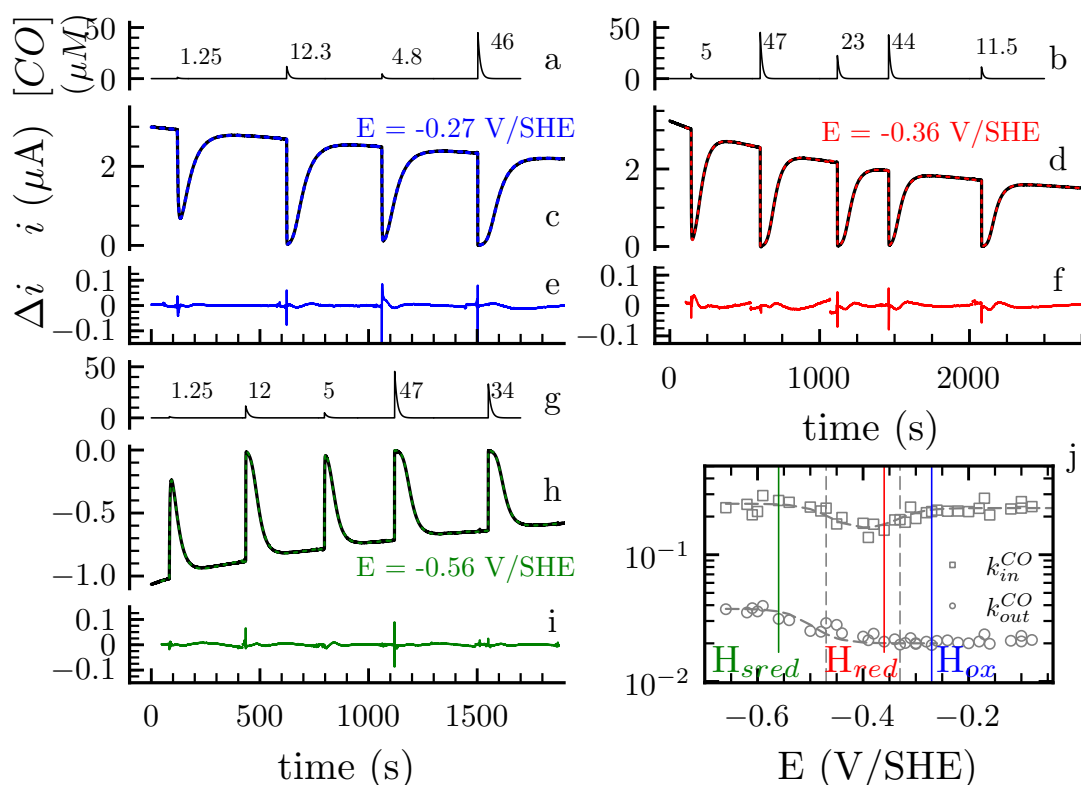


Figure S4: Kinetics of CO inhibition probed in chronoamperometry experiments upon repeated transient exposure to different initial CO concentrations under three oxidation states of the H-cluster. (a, b, g) CO concentration in the cell against time; (c, d, h) raw hydrogenase activity (black) and best fit of the parameters of scheme 1 (blue); (e, f, i) difference between fit and data; (j) position of the the data sets presented in panels c, d and h (blue, red and green lines, respectively) on the overall kinetic plot (main text Figure 5). Experimental conditions: pH 7, $[H_2] = 1$ atm, $T = 30$ °C, $\omega = 3$ *krpm*.

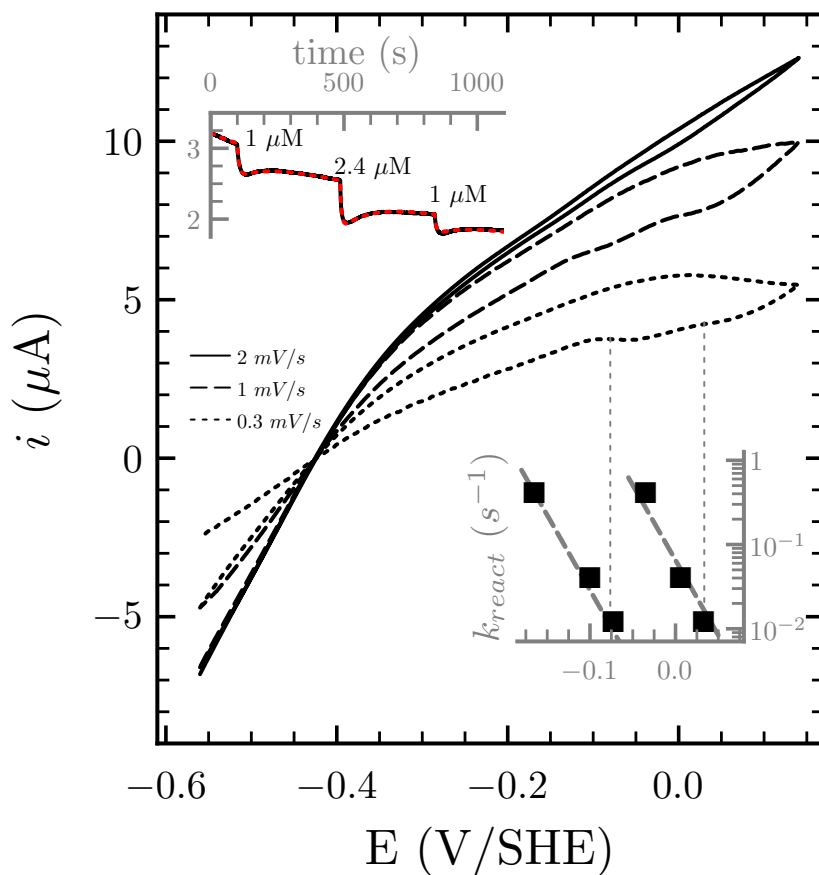


Figure S5: Oxidative (in)activation of HDCR in cyclic voltammetry at 12 °C. The position of the E_{switch} features was determined on the first derivative and the corresponding reactivation rate constants are plotted in the lower right inset. The value of k_{react} at high potential was used as an input for fitting kinetic traces (upper left panel) of aerobic inactivation upon transient O_2 exposure (black); the best fit of parameters of scheme 2 is shown in red. Experimental conditions: $[H_2] = 1 \text{ atm}$, $\text{pH } 7$, $\omega = 3 \text{ krpm}$.

References

- [1] K. Schuchmann and V. Müller, *Science*, 2013, **342**, 1382–1385.
- [2] E. T. Judd, M. Youngblut, A. A. Pacheco and S. J. Elliott, *Biochemistry*, 2012, **51**, 10175–10185.
- [3] B. Li and S. J. Elliott, *Electrochimica Acta*, 2016, **199**, 349–356.
- [4] V. Fourmond, *Anal. Chem.*, 2016, **88**, 5050–5052.
- [5] F. Leroux, S. Dementin, B. Burlat, L. Cournac, A. Volbeda, S. Champ, L. Martin, B. Guigliarelli, P. Bertrand, J. Fontecilla-Camps, M. Rousset and C. Léger, *Proceedings of the National Academy of Sciences*, 2008, **105**, 11188–11193.
- [6] P. Ceccaldi, E. Etienne, S. Dementin, B. Guigliarelli, C. Léger and B. Burlat, *Biochimica et Biophysica Acta (BBA) - Bioenergetics*, 2016, **1857**, 454–461.
- [7] P.-P. Liebgott, F. Leroux, B. A. A. Burlat, S. A. Dementin, C. Baffert, T. Lautier, V. Fourmond, P. Ceccaldi, C. Cavazza, I. Meynial-Salles, P. Soucaille, J. C. Fontecilla-Camps, B. Guigliarelli, P. Bertrand, M. Rousset and C. Léger, *Nature Chemical Biology*, 2009, **6**, 63–70.
- [8] Y. Nicolet, C. Piras, P. Legrand, C. E. Hatchikian and J. C. Fontecilla-Camps, *Structure*, 1999, **7**, 13–23.
- [9] V. Fourmond, C. Greco, K. Sybirna, C. Baffert, P.-H. Wang, P. Ezanno, M. Montefiori, M. Bruschi, I. Meynial-Salles, P. Soucaille, J. Blumberger, H. Bottin, L. De Gioia and C. Léger, *Nature Chemistry*, 2014, **6**, 336–342.
- [10] D. W. Mulder, M. W. Ratzloff, M. Bruschi, C. Greco, E. Koonce, J. W. Peters and P. W. King, *J. Am. Chem. Soc.*, 2014, **136**, 15394–15402.
- [11] A. Kubas, C. Orain, D. De Sancho, L. Saujet, M. Sensi, C. Gauquelin, I. Meynial-Salles, P. Soucaille, H. A. Bottin, C. Baffert, V. Fourmond, R. B. Best, J. Blumberger and C. Léger, *Nature Chemistry*, 2016, **advance online publication**, in–press.